

AN ANALYTICAL INVESTIGATION OF THE IMPINGEMENT
OF JETS ON CURVED DEFLECTORS

N. M. Schnurr*

J. W. Williamson⁺

J. W. Tatom[≠]

(NASA-CR-129136) AN ANALYTICAL
INVESTIGATION OF THE IMPINGEMENT JETS ON
CURVED DEFLECTORS N.M. Schnurr, et al
(Vanderbilt Univ.) [1972] 41 p CSCL 20D

N73-11252

G3/12 Unclas
16655

Vanderbilt University
Nashville, Tennessee

This work was supported by NASA Grant NGR-43-003-034. The authors wish to acknowledge the contributions of Larry J. Huey whose work led to the research reported here.

AIRCRAFT DECELERATION SYSTEMS

*Associate Professor of Mechanical Engineering

⁺Associate Professor of Mechanical Engineering

[≠]Associate Professor of Mechanical Engineering, Member AIAA

REPRODUCED BY
NATIONAL TECHNICAL
INFORMATION SERVICE
U.S. DEPARTMENT OF COMMERCE
SPRINGFIELD, VA 22161

ABSTRACT

Numerical solutions are obtained for the cases of straight circular jets impinging on axisymmetric curved surfaces and plane jets impinging symmetrically on two-dimensional curved surfaces. These geometries are representative of some types of thrust reversers for transport aircraft. The solutions are based on the assumptions of incompressible and potential flow. The velocity field, pressure distribution at the deflector surface and reverser effectiveness are predicted for deflector turning angles of 15° to 75° , deflector width to jet diameter ratios of 1.5 to 2.0, and ratios of deflector clearance to jet diameter of 1.0 to 3.0. Reverser effectiveness is found to be a maximum for a ratio of deflector clearance to jet diameter of about 2.0. The effect of back pressuring due to the presence of the deflector is predicted. Experimental verification of the theoretical predictions is obtained. A compressible solution obtained for a limited number of cases indicates that the incompressible solution is satisfactory for jet exit Mach numbers less than 0.8.

NOMENCLATURE

C	Local sonic velocity (ft/sec)
h	Deflector depth (ft)
L_1	Jet half width (ft)
L_2	Length of duct from which jet flows (ft)
L_3	Jet exit to deflector spacing (ft)
L_4	Reflector width (ft)
n	Normal distance (ft)
P	Pressure (lb/ft ²)
P_s	Static pressure (lb/ft ²)
P_∞	Ambient pressure (lb/ft ²)
s	Tangential distance (ft)
\vec{V}	Velocity (ft/sec)
V_s	Magnitude of the velocity along the free streamline (ft/sec)
x	Distance measured from the stagnation point normal to the jet symmetry line or plane (ft)
y	Distance measured from the stagnation point along the jet symmetry line or plane (ft)
η	Reverser effectiveness
η_T	Turning effectiveness

- θ Deflector turning angle
- ρ Fluid density (lb_m/ft^3)
- ϕ Dimensionless velocity potential = $\bar{\phi}/V_s L_1$
- $\bar{\phi}$ Velocity potential (ft^2/sec)

INTRODUCTION

The purpose of the work described in this paper is to provide an analytical method for predicting the flow field and resulting forces produced by the impingement of a jet on a curved surface. The shapes of the surfaces investigated are representative of a type of thrust reverser proposed for STOL and conventional aircraft. The analytical method is then used to predict the effects of several geometrical parameters on reverser performance.

The authors are not aware of any previous analytical solutions of jets impinging on curved surfaces. A variety of methods have been used to study the impingement of axisymmetric or plane jets on flat surfaces [1-6]*. In all of these analyses the flow was assumed potential and incompressible. The work which most closely approximates the case of a curved deflector is that of Chang and Conly [7] and Chang and Waidelich [8]. They used conformal mapping to solve the case of the deflection of an incompressible, two-dimensional jet by a series of straight segments of arbitrary number, length, and angles. This work is limited to incompressible plane jets of uniform velocity, however, and the effects of back pressuring are not included.

*Numbers in brackets designate references at end of paper.

The present authors have recently attempted to develop an analytical solution similar to that used by Shen [1] and apply it to the cases of a circular radial jet impinging on a hemispherical surface and a plane radial jet impinging on a cylindrical surface [9, 10]. Series solutions were obtained for both cases but were not satisfactory from a practical standpoint due to the extremely large size of the coefficients and erratic behavior in certain regions of the flow.

All of the analytical methods referred to above are limited to the simplest geometries and could not be applied to target thrust reversers of arbitrary shape. It is unlikely that a closed form solution applicable to a variety of thrust reverser shapes is possible and it appears that a purely numerical method is the best approach.

GEOMETRICAL CONFIGURATIONS

Analytical solutions were obtained for both straight circular jets impinging on axisymmetric curved surfaces and plane jets impinging symmetrically on two-dimensional curved surfaces. These two cases are illustrated in Figure 1 (a) and (b). The circular jet case (a) is representative of a type of thrust reverser which has received some consideration. The plane jet case (b) is not an exact representation of a practical target thrust reverser but is nevertheless of interest for several reasons. First of all, by proper selection of the shape, the deflector may correspond to a type of cascade thrust reverser, Figure 1 (c). Secondly, it may give at least qualitative information for the performance of the type of target thrust reverser shown in Figure 1 (d). Finally, case (b) is easier to duplicate experimentally for the purpose of checking the validity of the inviscid flow assumption used in the analysis.

It should be noted that most target thrust reversers produce three-dimensional flows (i.e. the velocity potential is a function of three independent space coordinates). A three-dimensional solution is exceedingly complex and beyond the scope of the present analysis. Nevertheless, the solutions reported here may be considered to be elements of most three-dimensional cases and may yield qualitatively useful results.

ANALYTICAL METHOD

The flow region to be analyzed is shown in Figure 2. This diagram serves for both the circular and plane jet cases with the distance L_1 being either the jet radius or half width depending on which case is being considered. The analytical procedure is discussed only for the plane jet solution since the procedure for the circular jet case is essentially the same with minor modifications to account for the different geometry.

The analysis is based on the assumptions of incompressible, inviscid and irrotational flow. Therefore, the flow field is completely specified when the velocity potential field is known. The governing differential equation for the velocity potential is the Laplace equation

$$\nabla^2 \bar{\phi} = 0$$

A dimensionless velocity potential may be defined as

$$\phi = \frac{\bar{\phi}}{V_s L_1}$$

where L_1 is the jet half width and V_s is the velocity at point C. The nondimensional velocity potential also satisfies Laplace's equation

$$\nabla^2 \phi = 0 \tag{1}$$

A complete solution is obtained by determining the potential function ϕ which satisfies equation (1) in the region in Figure 2 and satisfies all the required boundary conditions. The velocity at any point may then be found from:

$$\vec{V} = \text{grad } \phi \quad (2)$$

and the static pressure P_s may be calculated from Bernoulli's equation:

$$P_s + 1/2 \rho \vec{V}^2 = \text{const.} \quad (3)$$

It is assumed that the velocity profile in the duct at a distance L_2 upstream from the jet exit is uniform. Therefore

$$\frac{\partial \phi}{\partial y} = \text{constant along AB.}$$

Additional boundary conditions are

$$\frac{\partial \phi}{\partial n} = 0 \quad \text{along AF and BC where } n \text{ is the distance measured normal to the surface}$$

$$\frac{\partial \phi}{\partial n} = 0 \quad \text{at the deflector surface}$$

and

$$P = P_\infty \quad \text{along the line DE. } P_\infty \text{ is the ambient pressure.}$$

There are two independent boundary conditions which must be satisfied at the free boundary CD. The first is that this boundary be a

streamline. This condition may be stated mathematically as

$$\frac{\partial \phi}{\partial n} = 0 \quad \text{where } n \text{ is the distance normal to the streamline.}$$

Therefore, lines of constant potential intersect the free boundary at right angles. The other condition is that the pressure be equal to the ambient pressure. Application of Bernoulli's equation indicates that this is equivalent to specifying a constant velocity along the streamline.

The second condition for the free boundary is, then

$$\frac{\partial \phi}{\partial s} = V_s$$

where s is distance measured tangentially along the curve and V_s is the velocity along the freestream boundary.

The major difficulty in solving this type of problem arises from the fact that the location of the free streamline is unknown. The procedure used here is similar to a method which has been applied to flow in a Borda mouthpiece and flow past an orifice plate by Southwell and Vaisey [11]. This procedure may be summarized as follows. A first guess of the location of the freestream boundary is made. This original estimate need not be very accurate but should have the qualitatively correct shape. A rectangular mesh is then selected which is small enough to produce at least 200 node points. Additional node points are located at all intersections of the grid lines with the deflector and with

the free streamline. The values of velocity potential at the node points on the free boundary are determined by using the constant velocity condition along that line. The velocity potential is arbitrarily set equal to zero at point C and values of ϕ are computed at successive points along the boundary by using the relationship $\Delta\phi/\Delta s = V_s$ where s is the distance measured along the curve.

A relaxation solution is used to obtain the velocity potential at each node point in the flow field. It must then be determined whether the assumed free boundary is the correct one. The remaining condition which must be satisfied at the free boundary is that it be a streamline. A necessary and sufficient condition is that a streamline be everywhere normal to lines of constant ϕ .

The method of checking this condition may be explained with the aid of Figure 3. The slope (S1) of the free streamline at point 1 is computed in finite difference form. The ϕ value at point 1 is then compared to values at 2, 3, and 4. It must fall between the values at 2 and 3 or those at 3 and 4.* Linear interpolation is used to locate the point 1' which has the same value of velocity potential as point 1. The slope (S2)

*An exception may arise if the free boundary is nearly horizontal or has a positive slope. Such cases are handled in a similar fashion using node points below and to the right of the boundary point in question.

of a line normal to the line $l' - l$ is computed. If $S_1 = S_2$ at all points along the free boundary the solution is complete. If not, the difference in the slopes is used as a guide in reshaping the free streamline and the process is repeated until a suitable solution is obtained.

Several checks were made to insure that the solution was satisfactory. A criterion for sufficient relaxation was determined by carrying out an extremely large number of iterations for a fixed boundary shape. It was found that the relaxation was essentially complete when the change in ϕ for successive iterations was less than .002% for every node point in the grid. The necessary number of node points was determined by successively increasing the number of node points and comparing the solutions. About 15 divisions in both the x and y direction were sufficient.

The boundary shape adjusted in an orderly fashion and did not change appreciably after about ten iterations. The final solution was checked by plotting isopotential lines and streamlines for the entire flow field as well as the pressure distribution along the solid surface and jet symmetry line.

Before the analytical results are discussed, experimental verification of the analysis will be presented.

Experimental Program

The purpose of the experimental program was to examine the validity of the potential flow assumption. Therefore, it was necessary to determine deflector surface pressures, reverse thrust loads, and free streamline location for comparison with the analytical results.

A nozzle that would produce a uniform free jet exit velocity profile was designed and built. The deflector shapes which were investigated were:

1. a symmetrical deflector of constant radius of curvature,
2. an asymmetrical deflector intended to model a cascade thrust reverser.

Figure 4 illustrates the apparatus used in generating the two-dimensional jet. The flow of air was produced by a centrifugal blower. Air flow rate was closely controlled by a sliding cover valve located at the blower exit. The air flowed through a horizontal 15 inch square duct seven feet long before entering the convergent nozzle. The two-dimensional nozzle which was 15 inches long, was formed with an elliptical pattern and produced a straight jet 1.5 inches wide and 16 inches long. This represents an aspect ratio of 10.7. Because of the large area ratio between the inlet and exit of the nozzle (approximately 10), the jet was symmetrical about the centerline and nearly uniform. The variation in velocity across the center portion of the jet was less than 5%. Exit jet velocities of 250 fps could be attained.

Two of the deflector models tested were cylindrical with a radius of curvature of 13.5 inches and a height of 16 inches. One had a 45° turning angle and the other a 15° turning angle. Each of these had a plywood base covered with a surface of 1/16 inch thick plexiglas. Pressure taps were angularly spaced from the centerline to the edge of the deflector in the plane at the center of the deflector. The third deflector model consisted of a wood structure covered with a smooth aluminum sheet. The ends of these deflectors were covered to prevent any end flow and provision was made for the velocity probe to be inserted from the top.

All velocity measurements were made with United Sensor and Control Corporation yaw probes. These were used to determine the total pressure and static pressure with a strobotac, the fluid temperature at exit of the jet was measured by an iron-constantan thermocouple, and the axial thrust exerted on the deflector surface was measured by a BLH Electronics, Inc. load cell. The deflector surface pressures were used as an alternate method of determining the total thrust load.

Results from the cylindrical deflector with a radius of 13.5 inches and with an included angle of 30° are representative of the data obtained in the experimental study. In this test, static and total pressures throughout the field, deflector surface pressures, and the position of the edge of the jet were measured. Figure 5 shows the deflector surface pressures

in dimensionless form for direct comparison to the predicted values of the analytical method. The predicted values of pressure distribution are quite sensitive to the number of node points used. The three predicted curves were produced by using 90, 180 and 360 node points in generating solutions. The agreement between the experimental and predicted pressures was very good when 180 or more node points were used. Figure 6 shows a comparison between the measured position and the predicted position of the free streamline. Again, the agreement is excellent. The measured position was quite sharp, and could be determined easily. It is unfortunate that the edge of the jet could not be measured beyond the $x = 1.6$ inches position because of the limitations of the measuring instrumentation.

The last deflector shape investigated was the cascade thrust reverser model. A sketch of this model is presented in Figure 7. This reverser produced a deflector loading of 27 lb. at a flow rate of 2210 cfm. Since the angle of the deflector (θ) at exit was 54° , the ideal reversed thrust should have been 33.7 lb. The difference between these values indicates a significant amount of spillage has occurred, and indeed this result has been verified by making velocity traverses at the edge of the deflector. The dimensionless deflector pressure ratio is plotted in Figure 8 and compared with the analytical prediction. The predicted results are generally much higher and the maximum variation between the

experimental and the theoretical results is about 28%. The reason for this significant variation is separation that occurred in the curved portion of the deflector surface because of the large adverse pressure gradient. The size of the separation bubble was determined by flow visualization and is shown in Figure 7.

The experimental tests indicate that the potential flow assumption used in the analysis is justified for all two-dimensional cases which have favorable pressure gradients along the deflector surface. However, in those cases having adverse pressure gradients there is the likelihood that separation will occur and the analytical solution discussed here is inapplicable.

ANALYTICAL RESULTS

Solutions were obtained for a variety of geometries for both the plane jet and circular jet cases.* The shape selected for a cross section of the deflector was an ellipse having its center on the jet axis and passing through points F and E (see Figure 2). The additional requirement that the slope of the deflector be a fixed value ($\tan \theta$) at E makes the curve unique. The geometrical parameters which were specified include the non-dimensional distances L_2/L_1 , L_3/L_1 , L_4/L_1 and h/L_1 and the angle θ .

The results obtained for each case included the free streamline location, the velocity potential field, the velocity vector at each node point, the pressure distribution along the deflector surface and jet centerline, the turning effectiveness, and the reverser effectiveness, η . The turning effectiveness, η_T , is defined as the ratio of reverse thrust to the momentum flux measured at the cross section a distance L_2 upstream of the jet exit. It may be calculated by simply determining the angle through which the flow is turned. Comparison of actual turning effectiveness with the ideal turning effectiveness which would result if the flow left the deflector exactly parallel to the deflector surface is an indication of the spillage. The reverser effectiveness, η , is the ratio of reverse thrust to the momentum flux which would exist at the jet exit cross section in the absence of back pressuring effects (i.e., if the deflector were not present). It, therefore, includes the loss in thrust due

* These solutions are discussed in greater detail in reference 13.

to reduced flow caused by the back pressuring effect. The flow field and pressure distributions for a typical case for a circular jet are shown in Figures 9 and 10.

A series of runs was made for both the plane and circular jet cases to investigate the effects of geometry on performance. The results for all cases are summarized in Table 1. The effect of jet exit to deflector spacing is perhaps of most interest. The effect of this parameter on reverser performance is shown in Figure 11 for the round jet case. The turning effectiveness increases with decreasing jet to deflector spacing as expected since "spillage" is decreased. There is, however, an accompanying decrease in mass flow rate with decreased spacing causing an eventual decrease in reverser effectiveness.

Note that an optimum spacing occurs at a deflector to jet spacing of approximately two. Povolny, et al [12] experimentally investigated the effect of jet to deflector spacing for the case of a round jet impinging on a hemisphere. Although their case is not identical to the one considered here it is quite similar. They found an optimum spacing of about 1.8 diameters.

The effect of deflector width is shown in Figure 12. Note that there is little to be gained by increasing deflector width above about 1.75 diameters. This conclusion is also in agreement with Povolny's experimental results. Figure 12 also clearly illustrates the effect of back pressuring. A jet to deflector spacing of one diameter gives much better turning effectiveness than a spacing of two diameters but the higher back pressuring causes the reverser effectiveness to be lower.

TABLE 1 - ANALYTICAL RESULTS

CIRCULAR JET CASES

Case	L_2/L_1	L_3/L_1	L_4/L_1	h/L_1	$\theta(^{\circ})$	η_T	η
A-1	1.0	1.0	1.5	.5	45	.60	.40
A-2	1.0	1.5	1.5	.5	45	.54	.44
A-3	1.0	2.0	1.5	.5	45	.48	.45
A-4	1.0	2.5	1.5	.5	45	.44	.43
A-5	1.0	1.0	1.75	.5	45	.64	.45
A-6	1.0	1.5	1.75	.5	45	.60	.51
A-7	.10	2.0	1.75	.5	45	.56	.53
A-8	1.0	3.0	1.75	.5	45	.43	.42
A-9	1.0	1.0	2.0	.5	45	.66	.49
A-10	1.0	1.5	2.0	.5	45	.63	.55
A-11	1.0	2.0	2.0	.5	45	.59	.57
A-12	1.0	3.0	2.0	.5	45	.55	.54
A-13	2.0	1.0	2.0	.5	45	.66	.49
A-14	1.0	1.5	1.75	.5	60	.75	.64
A-15	1.0	1.5	1.75	.5	30	.42	.36
A-16	1.0	1.5	1.75	.5	75	.86	.73

PLANE JET CASES

B-1	2.0	2.0	2.0	.34	15	.19	.13
B-2	2.0	2.0	2.0	.34	30	.38	.28
B-3	2.0	2.0	2.0	.34	45	.53	.39
B-4	2.0	2.0	3.0	.80	30	.47	.34
B-5	2.0	3.0	3.0	.80	30	.45	.40
B-6	2.0	4.0	3.0	.80	30	.43	.41
B-7	2.0	5.0	3.0	.80	30	.41	.40

The effect of turning angle is illustrated in Figure 13. As θ increases both the turning effectiveness and reverser effectiveness increase monotonically. The back pressuring loss shows essentially no increase with turning angle for the geometry considered here.

The purpose of including a length of duct L_2 was to investigate the effect of back pressuring. Since the resulting straight section of duct may not be representative of practical cases, the effect of L_2/L_1 was not studied exhaustively. It was assumed that increasing L_2/L_1 beyond 1.0 would have little effect on the predicted performance. The validity of this assumption is demonstrated by comparison of cases A-9 and A-13 in Table 1.

The results discussed above were obtained using the incompressible equations for potential flow. The effect of compressibility was investigated for a few cases for the round jet by using the compressible flow equations for potential flow

$$\left(1 - \frac{\phi_r^2}{c^2}\right) \phi_{rr} + \left(1 - \frac{\phi_z^2}{c^2}\right) \phi_{zz} - \left(2 \frac{\phi_z \phi_r}{c^2}\right) \phi_{rz} + \frac{\phi_r}{r} = 0$$

where c is the local sonic velocity and subscripts indicated partial differentiation with respect to that variable. This equation was converted to finite difference form and some linearizing approximations were made so that it could be solved explicitly for the velocity potential at a point as a function of the potential at surrounding node points. The added complexity of these

equations caused a substantial increase in computer time so that only one case was solved for various values of reference Mach number, M . The reference Mach number was based on the velocity V_s and a static temperature of 70°F . It was found that the cases for $M = .1$ and $.5$ yielded results extremely close to those obtained using the incompressible equations. At $M = .8$ some deviation in the pressure distribution along the deflector surface was noted (see Figure 14) but the difference in reverser effectiveness was still within about 1% of the incompressible results. This indicates that the incompressible results are adequate up to $M = .8$. This conclusion is not unexpected in view of the fact that the specified Mach number applies to the free streamline where the velocity is highest, and the Mach number throughout most of the flow field is significantly lower.

CONCLUSIONS

A numerical method has been developed to predict the flow field and reverse thrust for the cases of straight circular jets impinging on axisymmetric curved surfaces and plane jets impinging symmetrically on two-dimensional curved surfaces. The method is much more flexible than previous analytical solutions since it can be used for a wide range of geometries, can include effects of back pressuring, and can be extended to compressible flow cases.

The inviscid flow assumption has been experimentally verified. Compressibility effects have been shown to be unimportant for jet exit Mach numbers less than .8. Results have been presented for a range of geometrical parameters. The effect of these parameters on reverser performance are:

1. Reverser effectiveness increases monotonically with deflector width but there is little further increase as the ratio of deflector width to jet diameter is increased above 1.75.
2. Reverser effectiveness increases monotonically with increased turning angle, θ . The turning angle has negligible effect on back pressuring for the range of geometries considered here.

3. Reverser effectiveness is a maximum for a ratio of deflector clearance to jet diameter of about 2.0. Closer spacing results in decreased flow rate caused by the back pressuring effect.

REFERENCES

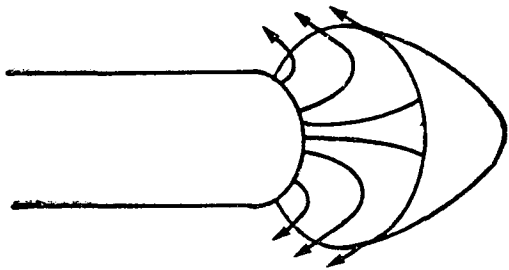
1. Shen, Y. C., "Theoretical Analysis of Jet-Ground Plane Interaction," IAS Paper No. 62-144, presented at the IAS National Summer Meeting, Los Angeles, California, June 19-22, 1962.
2. Strand, T., "Inviscid-Incompressible-Flow Theory of Static Two-Dimensional Solid Jets in Proximity to the Ground," Journal of the Aerospace Sciences, Vol. 29, No. 2, pp. 170-184, February, 1962.
3. Brady, W. G., and Ludwig, Gary, "Theoretical and Experimental Studies of Impinging Uniform Jets," IAS Paper No. 63-29, presented at the IAS 31st Annual Meeting, New York, New York, January 21-23, 1963.
4. Brady, W. G., and Ludwig, Gary, "Theoretical and Experimental Studies of Impinging Uniform and Non-Uniform Jets," Cornell Aeronautical Laboratory Report TG-1818-S-1, August, 1964, Ithica, New York.
5. Schach, W., "Umlenking eines Kreisformigen Flussigkeitsstrahles and einer ebenen Platte Senkrecht zur Stromungsrichtung," (Deflection of a Circular Fluid Jet by a Flat Plate Perpendicular to the Flow Direction), Ingenieur-Archiv, Vol. VI, pp. 51-59, 1935.

6. Milne-Thomson, L. M., *Theoretical Hydrodynamics*, 5th Ed.,
The Macmillan Company, 1950, New York, New York.
7. Chang, H. Y., and Conly, J. F., "Potential Flow of Segmental
Jet Deflectors," Journal of Fluid Mechanics (1971), Vol. 46,
Part 3, pp. 465-475.
8. Chang, H. Y., and Waidelich, J. P., "A Mathematical Model for
the Behavior of Thrust Reversers," Journal of Aircraft, Vol. 7,
No. 2, p. 164, March, 1970.
9. Huey, Larry J., "An Analytical Investigation of Jets Impinging on
Curved Surfaces," M.Sc. Thesis, Department of Mechanical
Engineering, Vanderbilt University, Nashville, Tennessee,
May, 1970.
10. Tatom, J. W., et al., "A Study of Jet Impingement on Curved
Surfaces Followed by Oblique Introduction into a Freestream
Flow," First Annual Report under NASA Grant NGR-43-002-034,
April, 1971.
11. Southwell, R. V., and Vaisey, G., "Relaxation Methods Applied
to Engineering Problems; XII. Fluid Motions Characterized
by Free Streamlines," *Phil. Trans. of the Royal Society*,
Ser. A., Vol. 240, 1946, pg. 117.
12. Povolny, et al., "Summary of Scale-Model Thrust Reverser
Investigation," NACA Report 1314.

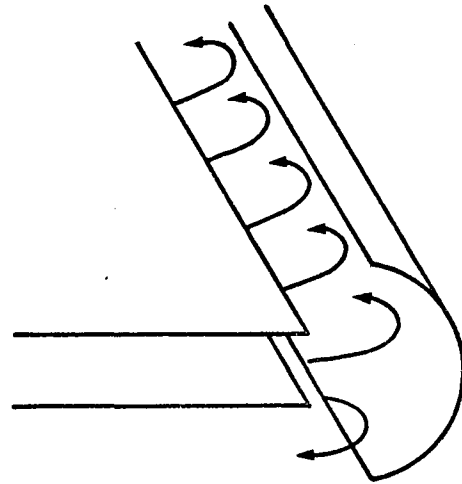
13. Tatom, J. W., et al., "A Study of Jet Impingement on Curved Surfaces Followed by Oblique Introduction into a Freestream Flow," Second Annual Report Under NASA Grant, NGR-43-002-034, February, 1972.

CAPTIONS FOR ILLUSTRATIONS

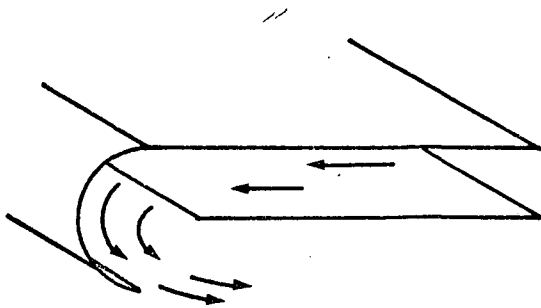
- Figure 1. Thrust reverser configurations .
- Figure 2. Jet impingement flow field .
- Figure 3. Illustration of boundary adjustment procedure .
- Figure 4. Schematic diagram of jet impingement test apparatus .
- Figure 5. Deflector surface pressure distribution .
- Figure 6. Free streamline location, 15° turning angle .
- Figure 7. Cascade thrust reverser flow field .
- Figure 8. Pressure distribution at the surface of the cascade thrust reverser .
- Figure 9. Velocity potential field for case A-6 .
- Figure 10. Pressure distributions for case A-6 .
- Figure 11. The effect of jet exit to deflector spacing on reverser performance .
- Figure 12. The effect of deflector width on reverser performance .
- Figure 13. The effect of turning angle on reverser performance .
- Figure 14. The effect of compressibility on pressure distribution at deflector surface .



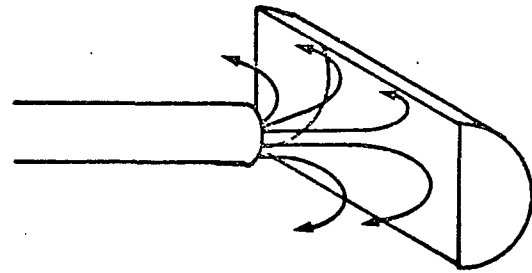
(a) CIRCULAR JET -
AXISYMMETRIC
DEFLECTOR



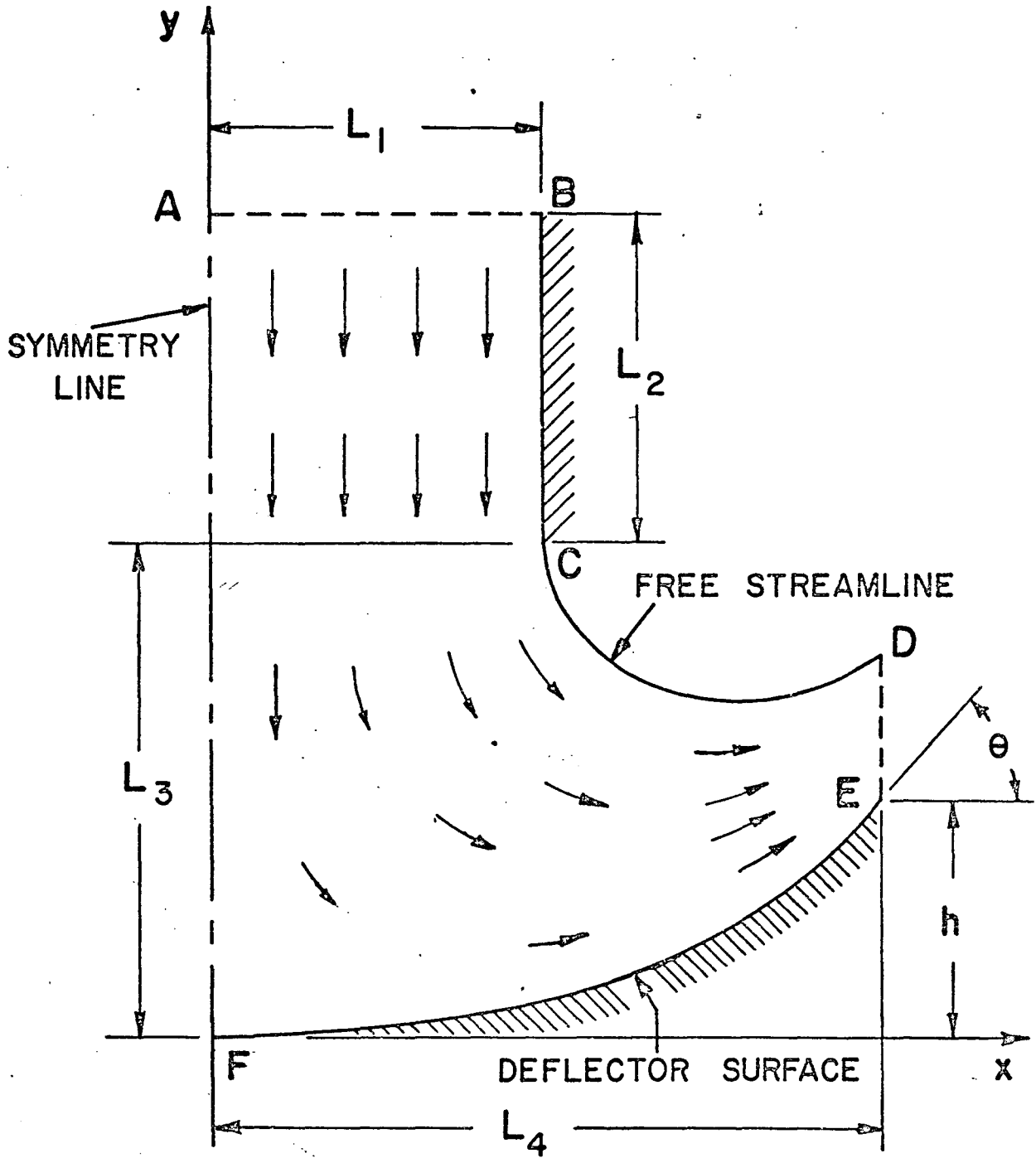
(b) PLANE JET - TWO
DIMENSIONAL DEFLECTOR



(c) CASCADE REVERSER



(d) CIRCULAR JET -
CURVED DEFLECTOR



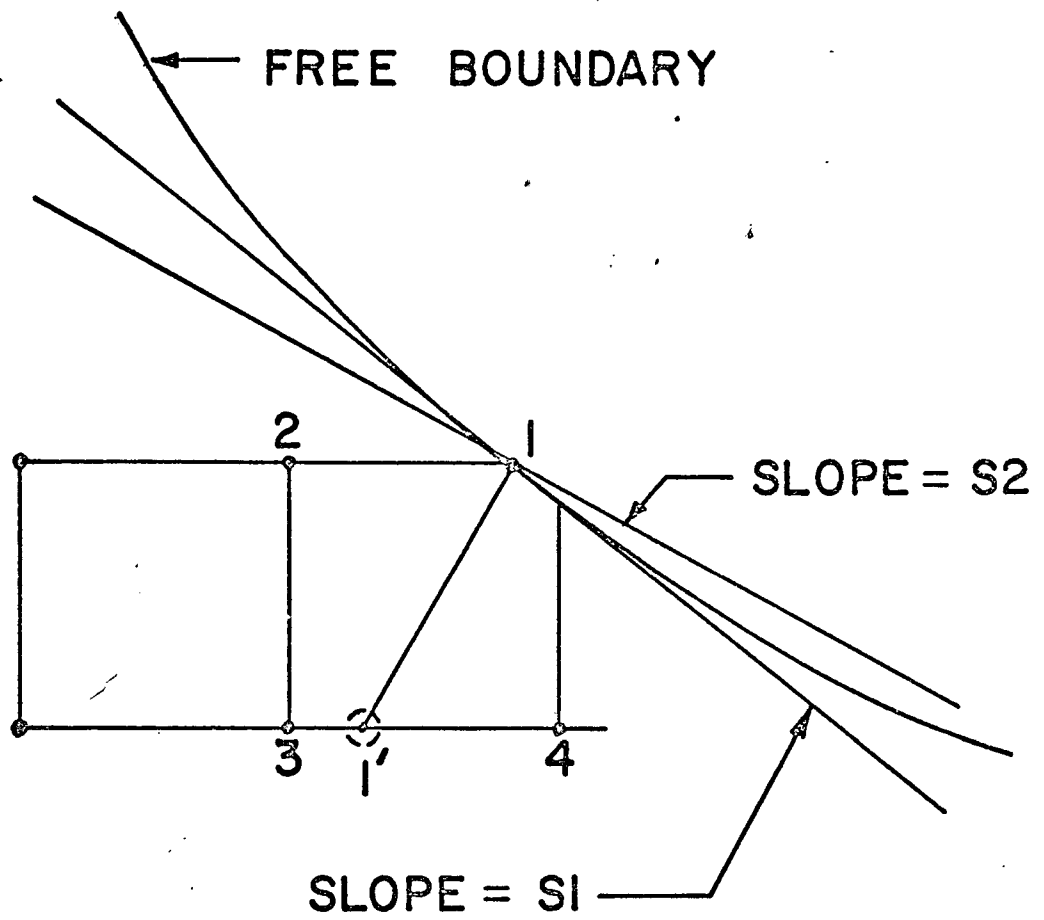
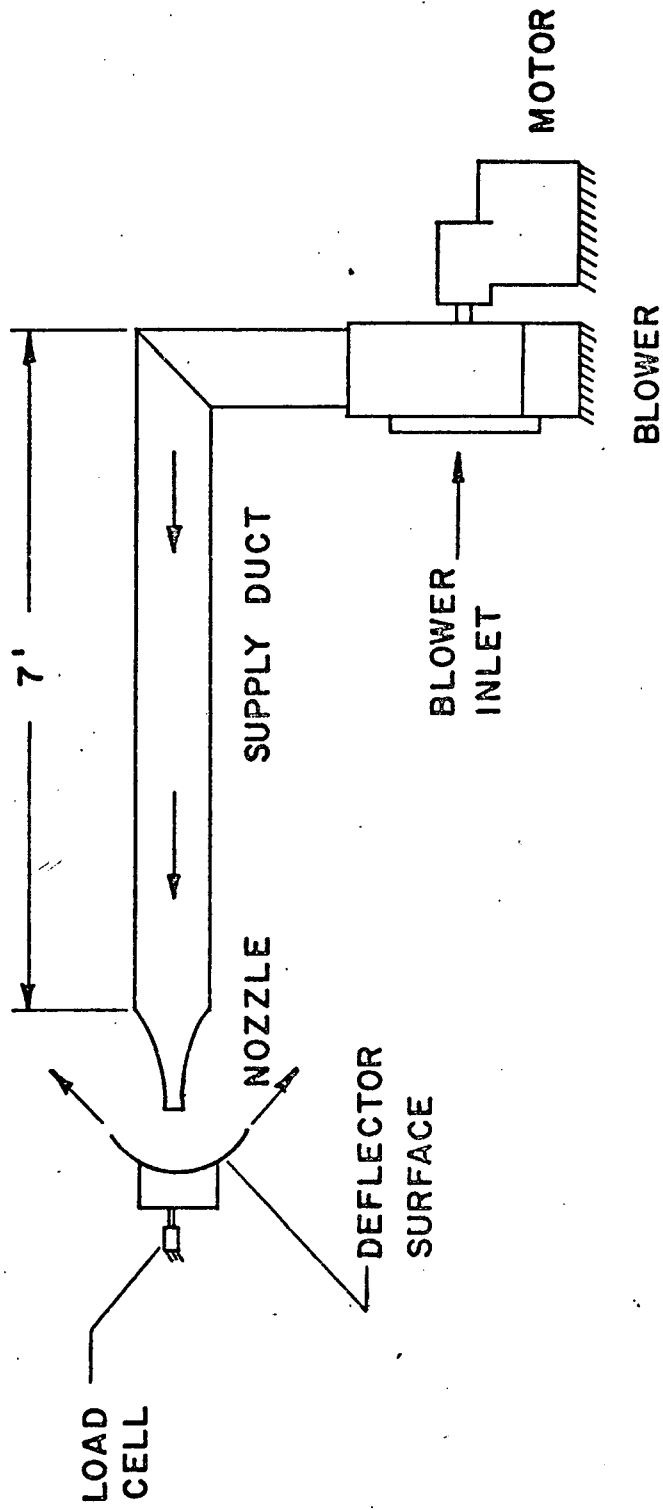
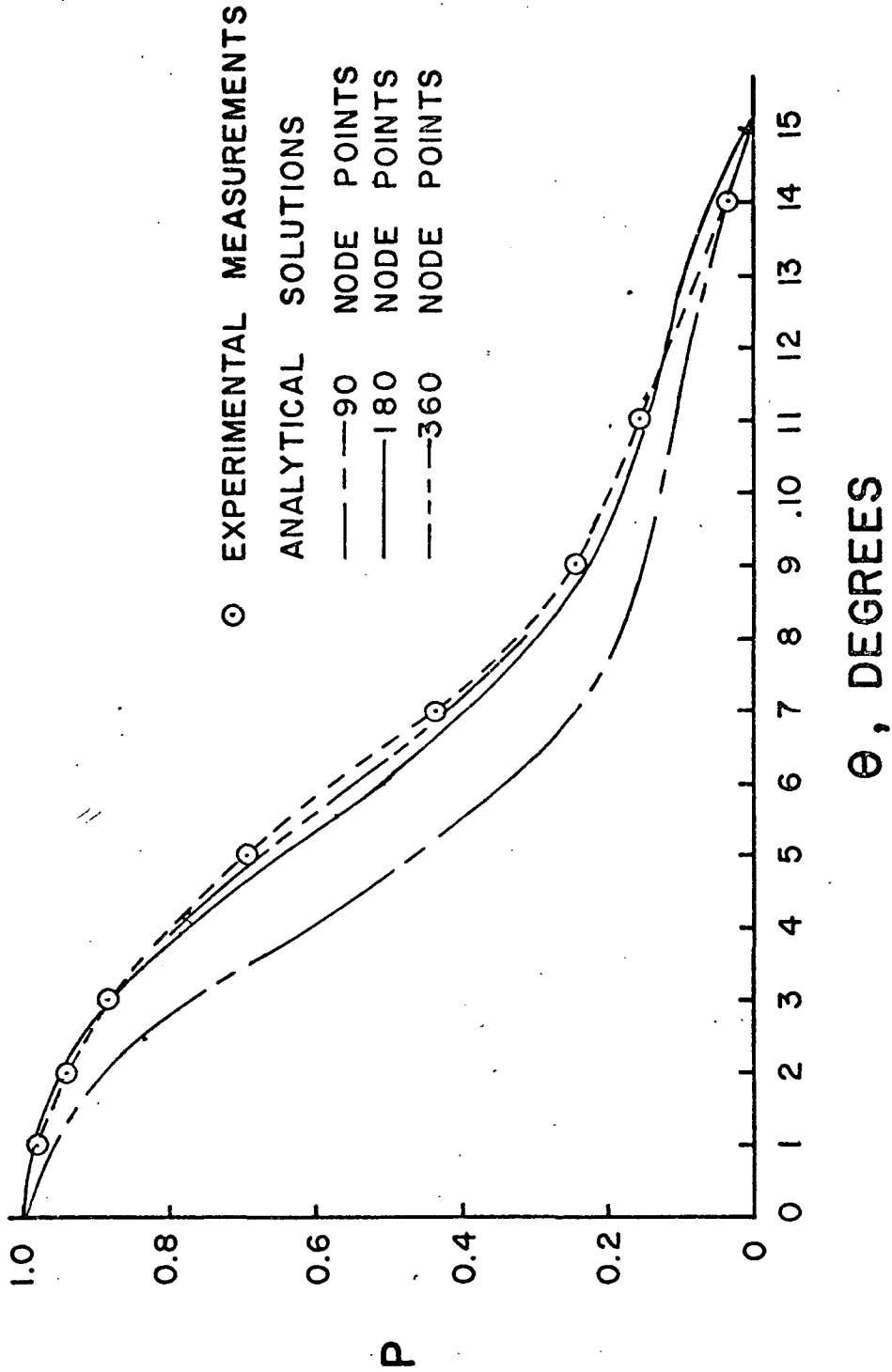


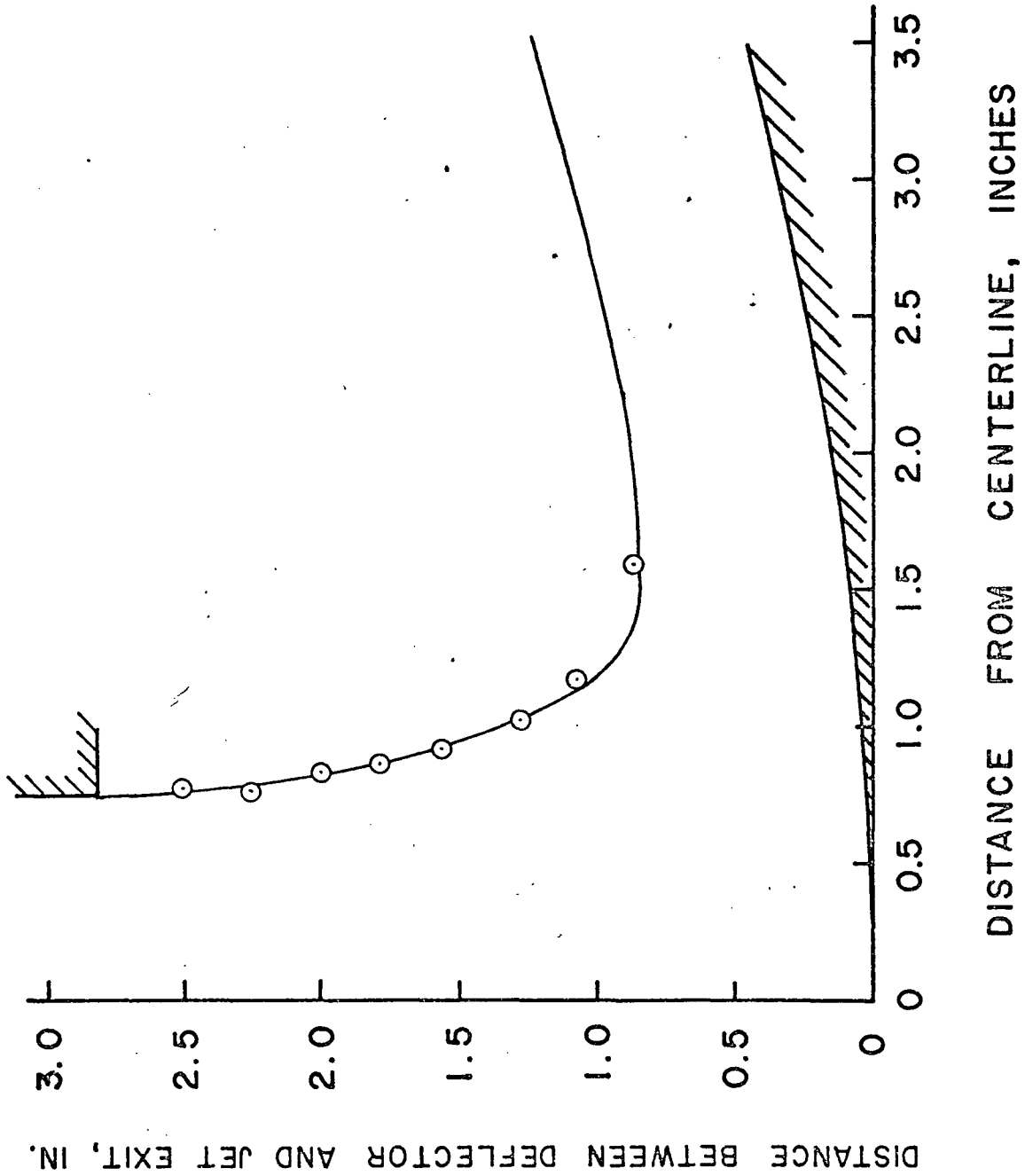
FIG III

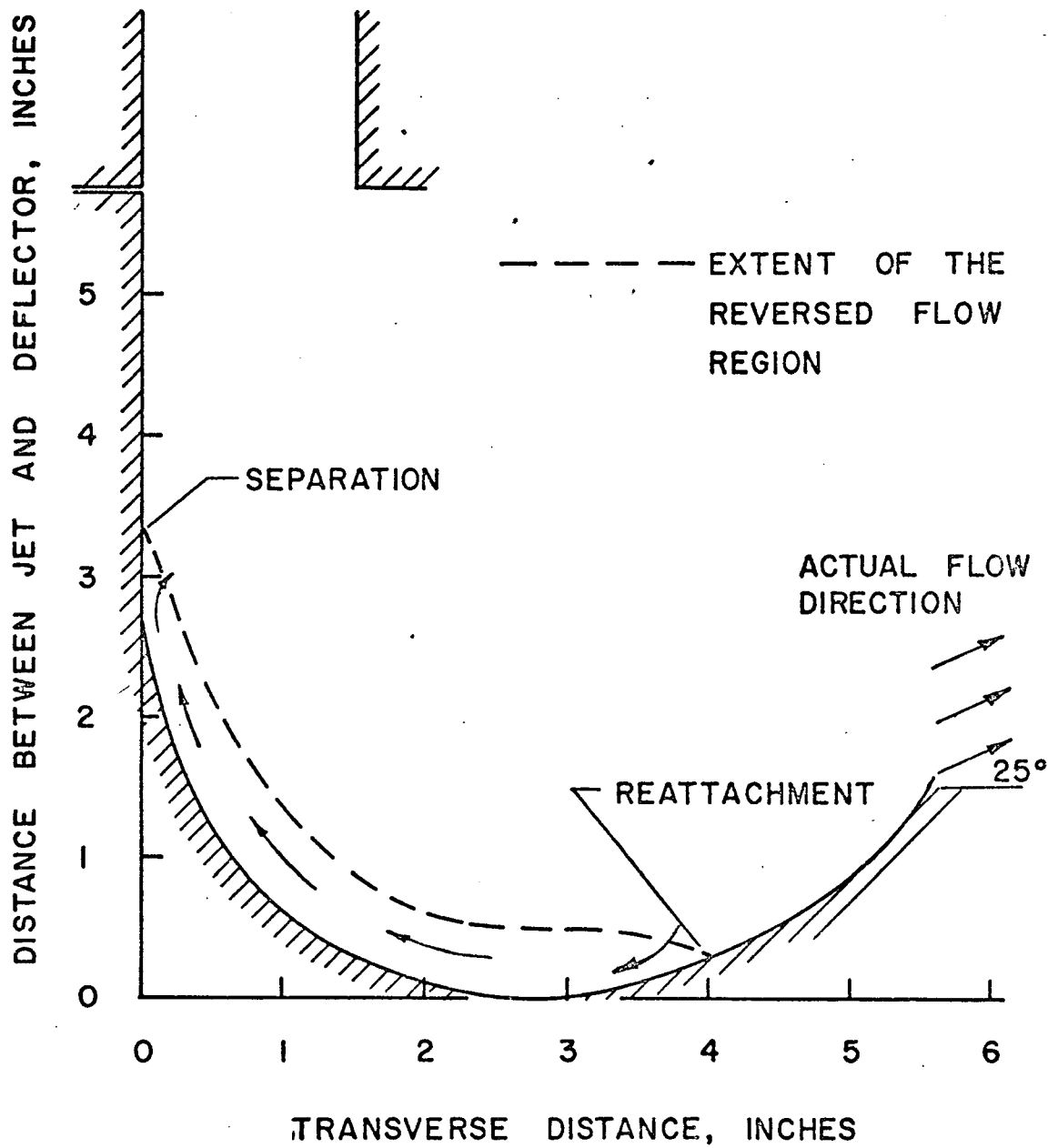


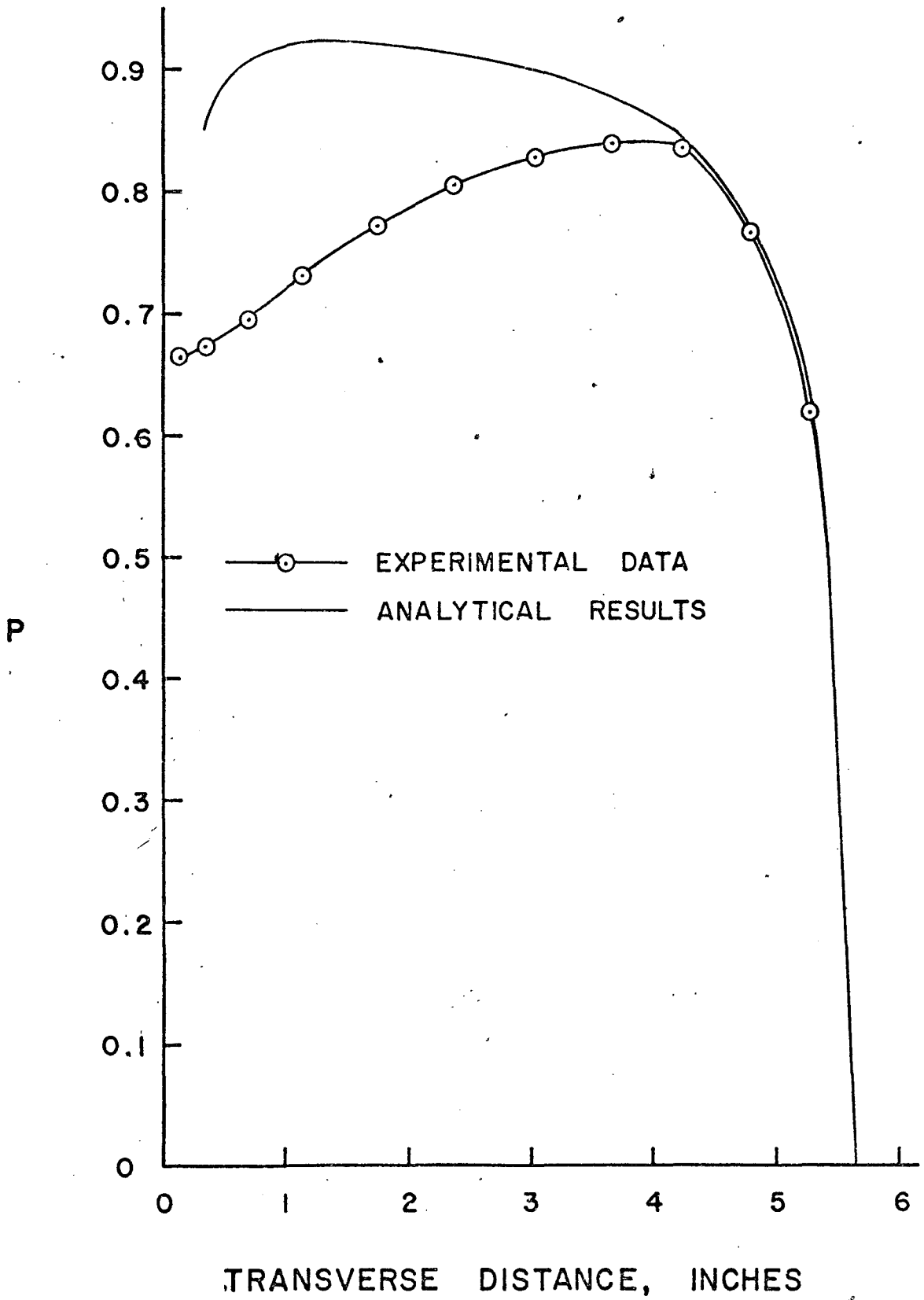
27

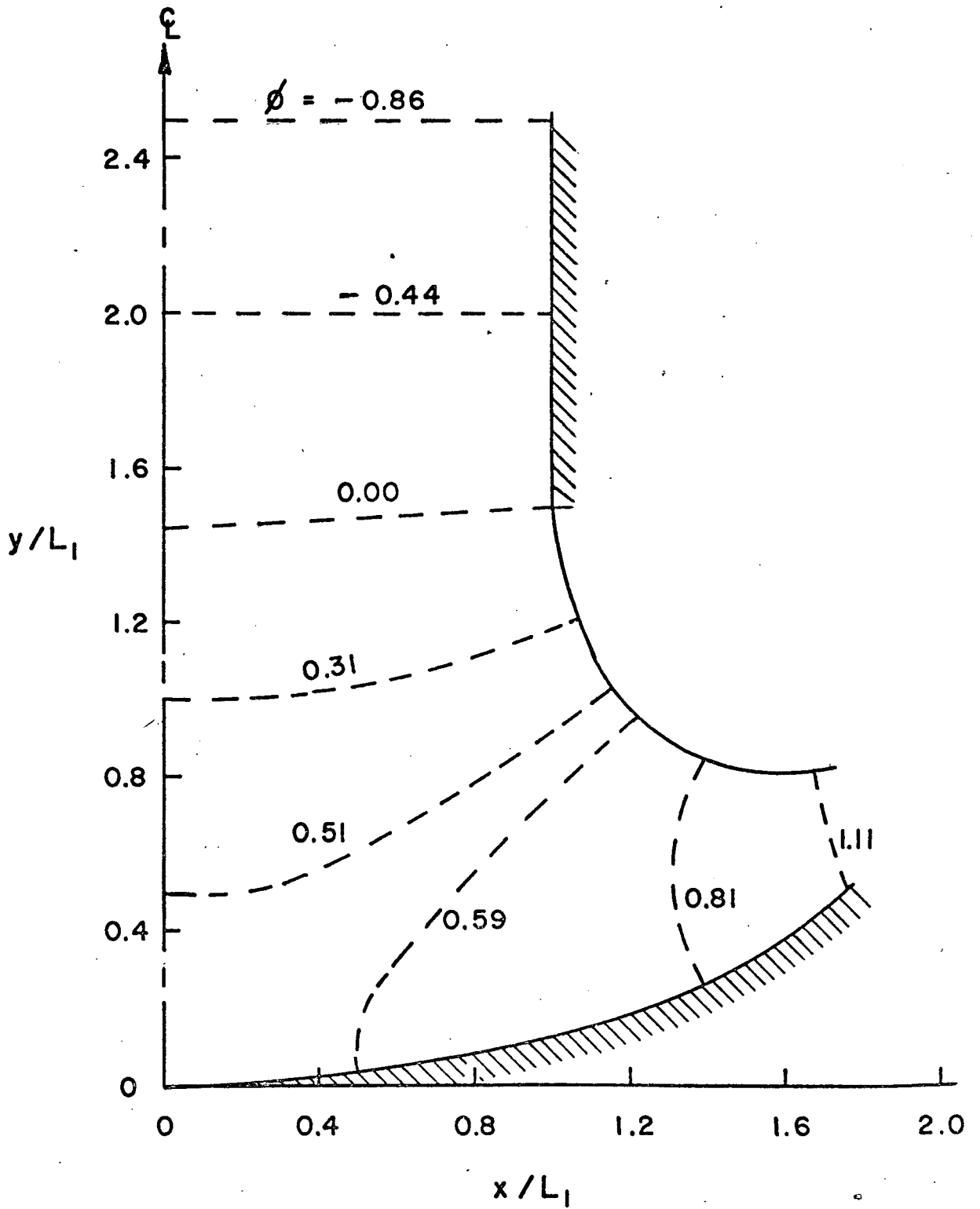
FIG. 11

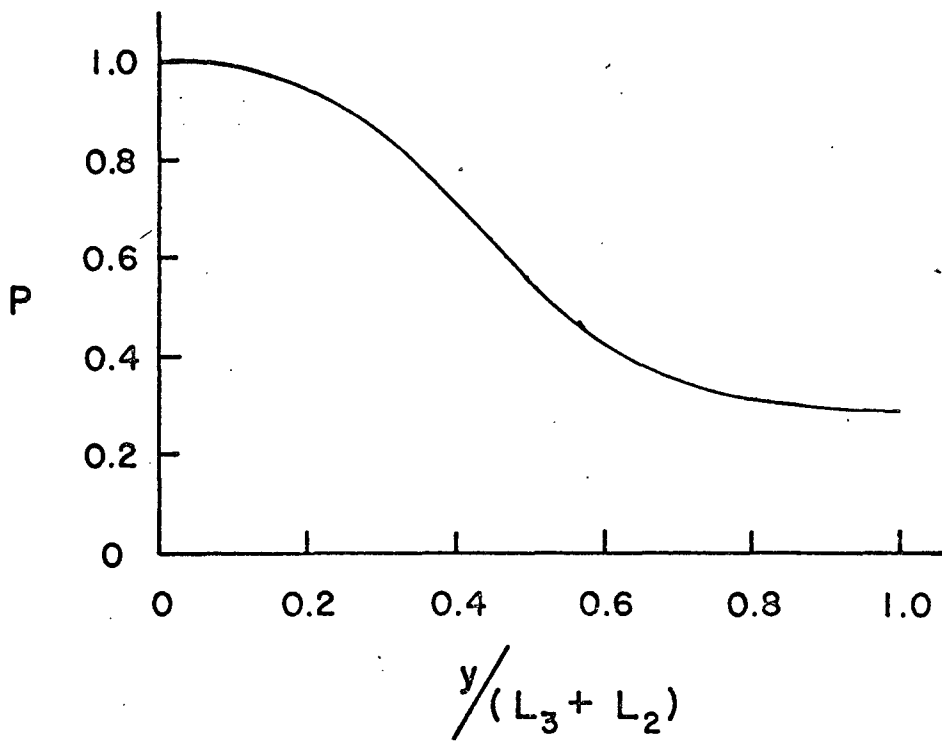
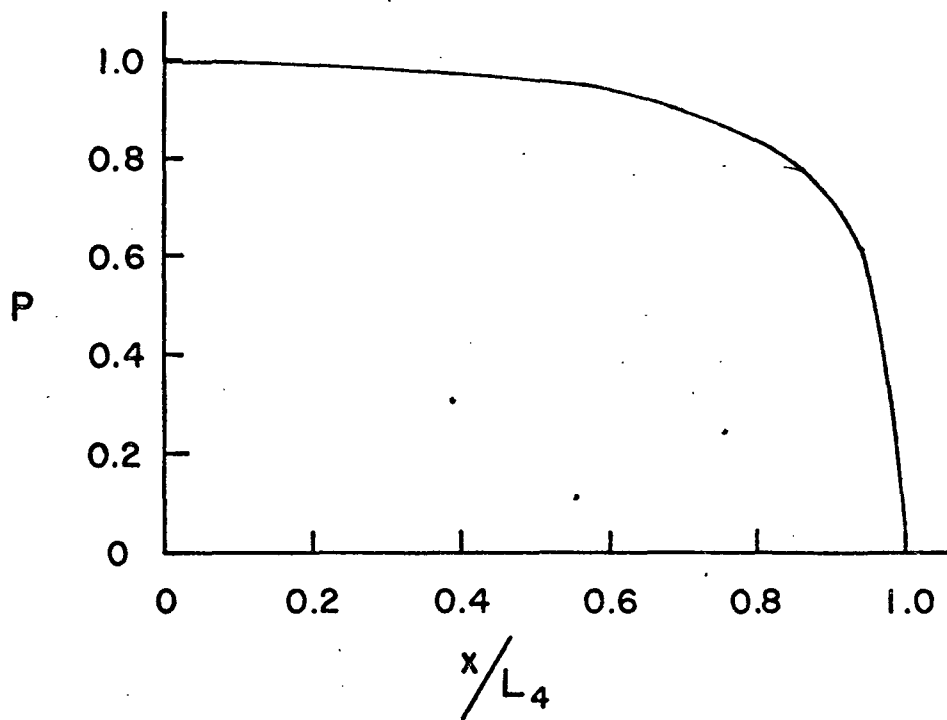


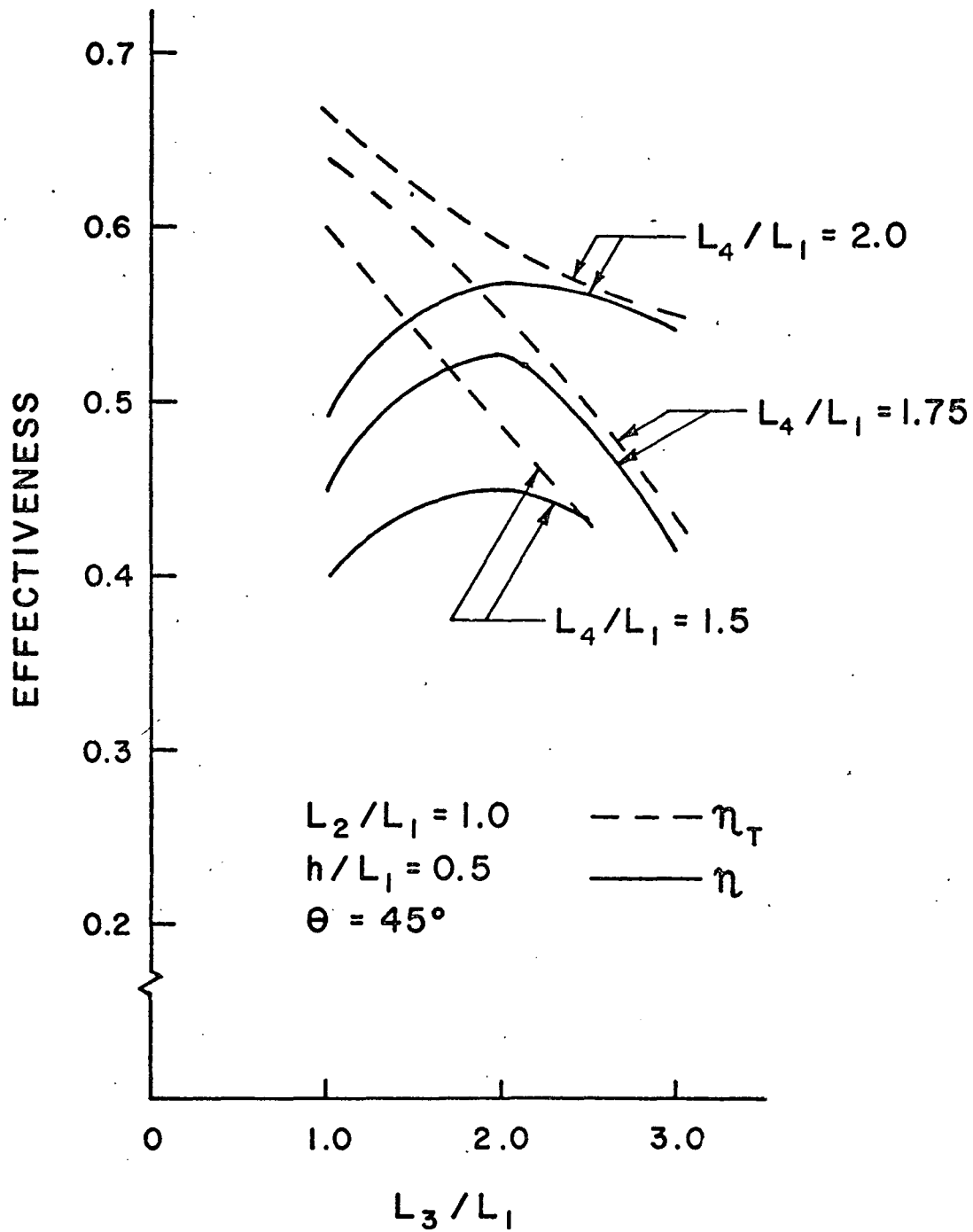






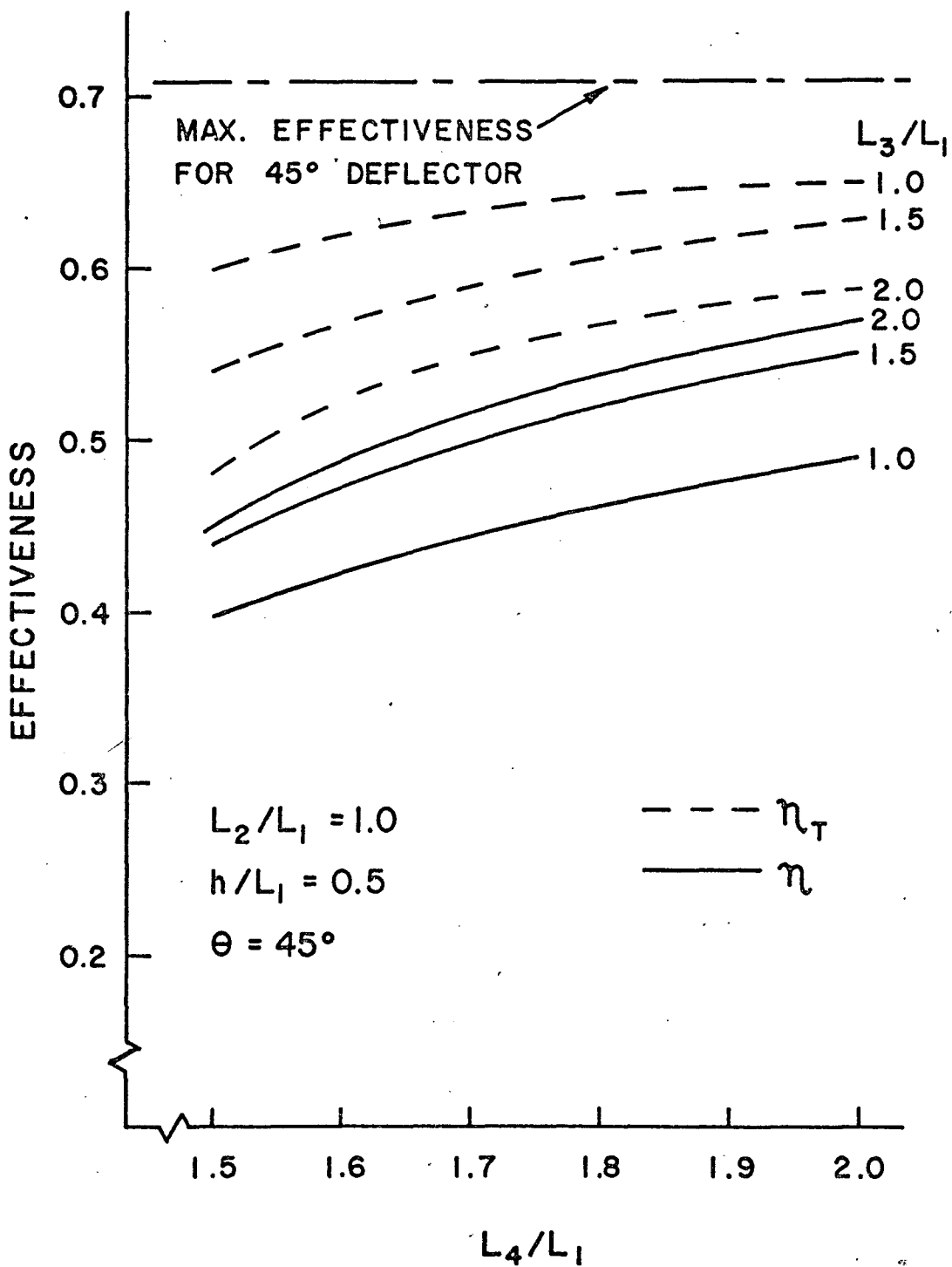






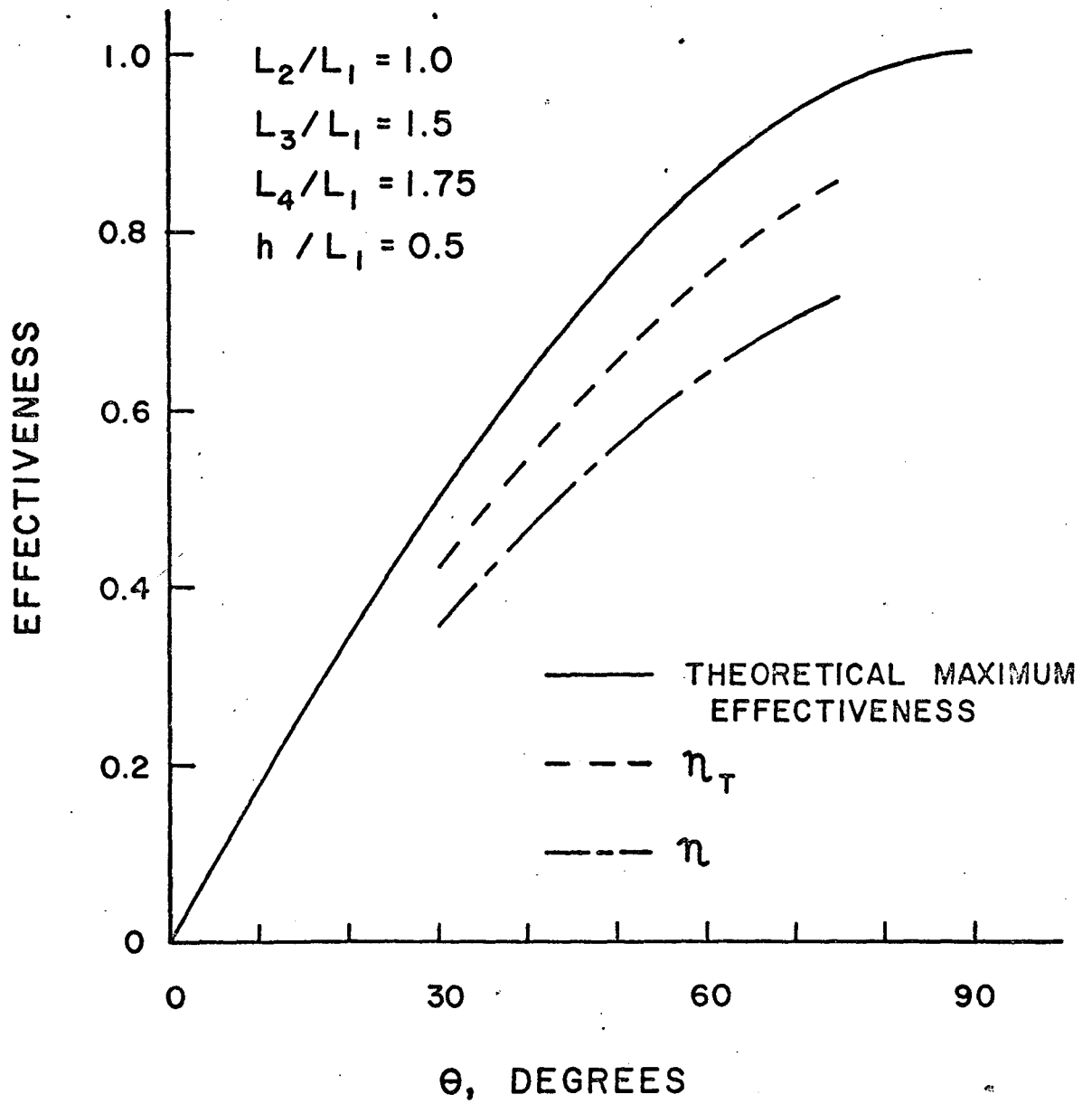
34

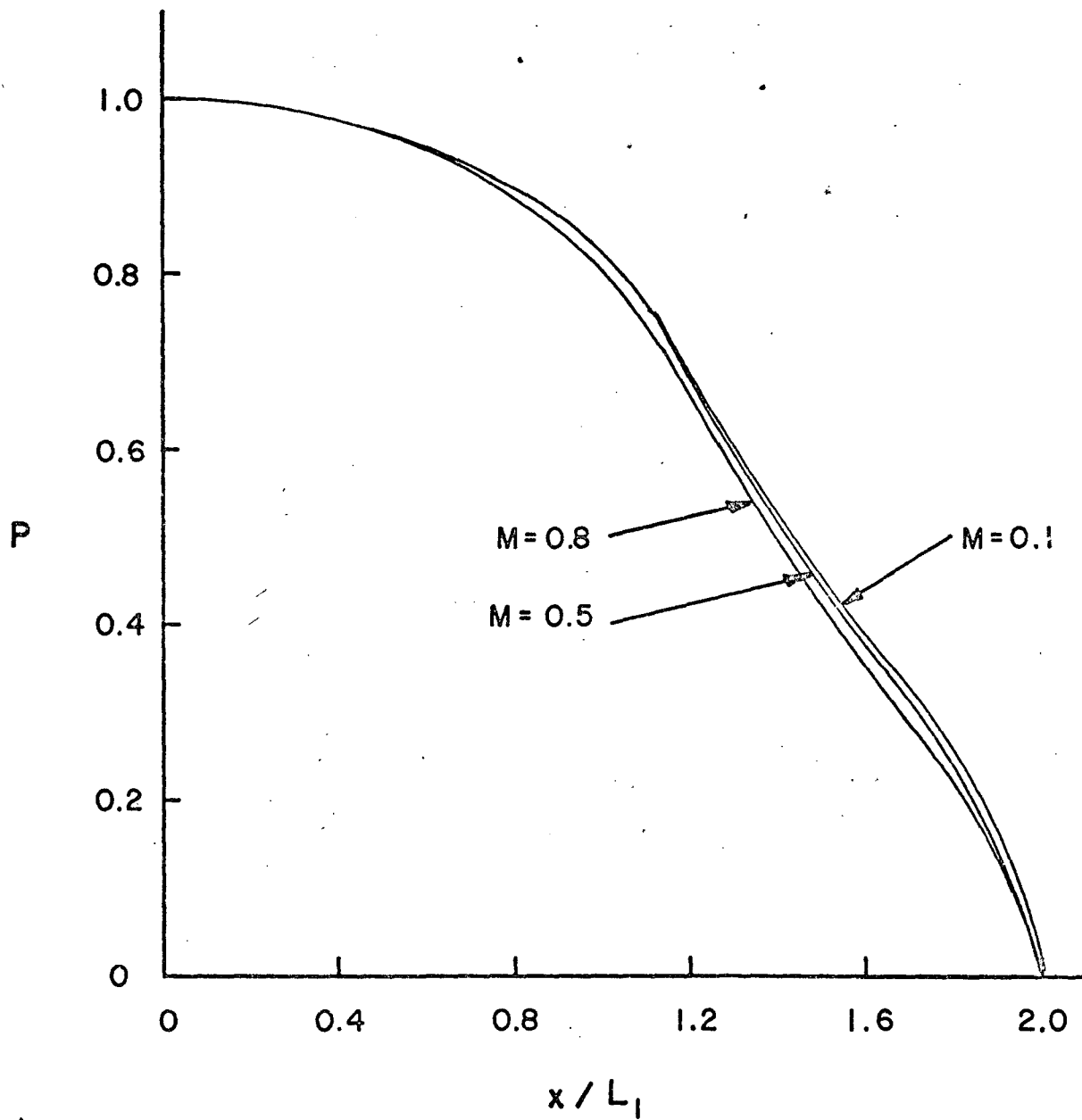
FIG II



35

FIG. 27





37

FIG. III